Density Functional Theory Study on the Reaction Mechanisms of Bis(cyclopentadienyl)magnesium with Hydrogenated and Hydroxylated Si(100)-(2×1) Surfaces

Hong-Liang Lu,* Shi-Jin Ding, and David Wei Zhang*

State Key Laboratory of ASIC and System, Department of Microelectronics, Fudan University, Shanghai 200433, People's Republic of China

Received: May 1, 2009; Revised Manuscript Received: June 11, 2009

The mechanisms for reaction between bis(cyclopentadienyl)magnesium and Si(100)-(2×1) surface are investigated with the aid of density functional theory calculations. The reactions on hydrogenated and hydroxylated Si surfaces are compared to understand the dominated initial reaction during atomic layer deposition of MgO on Si surface. The overall reaction energy and activation barrier are calculated for each reaction. It is found that the reaction of bis(cyclopentadienyl)magnesium with OH-terminated Si surface is both kinetically and thermodynamically more favorable than that with H-terminated Si surface.

1. Introduction

Magnesium oxide (MgO) is attracting much research interest because of its refractory and insulating nature, wide band gap, and diffusion barrier properties.[1−3] MgO films can be used in several applications such as barrier layers in Josephson tunnel junctions,[4] buffer layers for growing oriented high-T_c superconducting films,[5] and protective layers in plasma display panels.[6] In addition, MgO has a dielectric constant of about 9.8 and a bulk band gap of 7.3 eV, which thus makes it a potential candidate to replace SiO_2 as the gate dielectric layer in advanced transistor fabrication.[7,8]

A number of deposition techniques have been used to prepare MgO thin films including chemical vapor deposition,[9] rf sputtering,[10] and sol−gel processes.[11] MgO thin films have also been deposited by atomic layer deposition (ALD),[12−14] which is a thin film growth method based on sequential, self-limiting surface chemical reactions. Huang and Kitai deposited MgO thin films on Si(111) substrates by ALD using $Mg(C_2H_5)_2$ and H_2O.[12] In the temperature range of 600−900 °C, the growth rate of the MgO film was 1.8−2.4 Å/cycle. MgO thin films were also deposited on Si(100) substrates by ALD from $Mg(thd)_2$ (thd = $C_{11}H_{19}O_2$) and ozone (O_3).[13] A narrow temperature range of 225−250 °C was found where the growth was surface-controlled with a growth rate of 0.22 Å/cycle. Moreover, ALD of MgO films on Si(100) using bis(cyclopentadienyl)magnesium ($Mg(Cp)_2$, Cp = C_5H_5) and H_2O in the temperature range of 125−400 °C has been done by Putkonen et al.[14] A plateau of surface-controlled growth was observed at 200−300 °C with a growth rate of 1.16 Å/cycle, which is about 1 magnitude higher than the ALD growth rate obtained with $Mg(thd)_2$ and O_3.

Formation of structures on the atomic scale requires an atomic- and molecular-level understanding of the reactions occurring during the process. Initial ALD reactions between metal precursors (e.g., trimethylaluminum, $HfCl_4$, and $ZrCl_4$) and silicon surfaces have been intensively investigated both experimentally and theoretically.[15−19] However, as an important class of organometallic compounds, the nature of the interaction of bis(cyclopentadienyl)-based metallocenes onto the silicon surface, the detailed geometry of its adsorption configurations, and the features of the dissociation processes possibly occurring upon adsorption are not yet fully understood. In spite of the above experimental activity, to our knowledge, no theoretical work has been performed on the adsorption and dissociation of $Mg(Cp)_2$ on the silicon surface. Accurate theoretical investigation could provide invaluable insights into the chemisorption of $Mg(Cp)_2$ on the silicon surface. Understanding the growth mechanism of the initial layer during ALD can help us to optimize the process conditions and to control the interface formed between the deposited film and silicon substrate.

In this work, first-principles calculations based on density functional theory are used to investigate the adsorption and dissociation configurations of $Mg(Cp)_2$ on the H- and OH-terminated Si(100)-(2×1) surfaces during initial MgO ALD reaction. A significant distinction for the reaction of $Mg(Cp)_2$ with H-terminated versus OH-terminated Si surface is obtained.

2. Computational Details

We have focused on the first critical half-cycle reaction that takes place during the initial step of atomic layer deposition of MgO films, i.e., the decomposition of $Mg(Cp)_2$ on Si−H* and Si−OH* surfaces

$$Mg(Cp)_2 + Si{-}H^* \rightarrow Si{-}MgCp^* + HCp \quad (R1)$$

$$Mg(Cp)_2 + Si{-}OH^* \rightarrow Si{-}O{-}MgCp^* + HCp \quad (R2)$$

where the asterisks denote surface species.

To investigate the reaction mechanisms and to calculate the energies for the surface reaction, a Si_9H_{12} cluster has been used to model the reconstructed Si(100)-(2×1) surface. The cluster includes a pair of surface-layer silicon atoms representing the dimer structure, 4 second-layer Si atoms directly bonded to the dimer atoms, 2 third-layer Si atoms, and 1 fourth-layer Si atom. The subsurface silicon atoms in the cluster are terminated with hydrogen atoms to avoid dangling bond effects. Such a finite

* Authors to whom correspondence should be addressed. Tel/Fax: +86 21 65642389. E-mail: honglianglu@fudan.edu.cn; dwzhang@fudan.edu.cn.

10.1021/jp904048d CCC: $40.75
Published on Web 07/02/2009

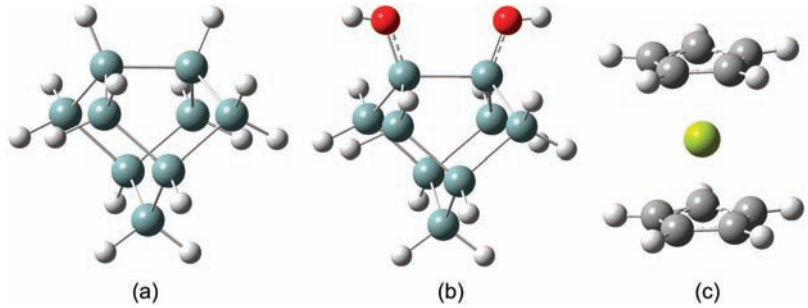

Figure 1. Structures of the Si_9H_{14} (a), $Si_9H_{14}O_2$ (b), and $Mg(C_5H_5)_2$ (c) clusters used to represent Si−H* surface, Si−OH* surface, and bis(cyclopentadienyl)magnesium, respectively. Blue, red, yellow, gray, and white balls represent Si, O, Mg, C, and H atoms, respectively.

cluster model of this type predicts energies and geometries in good agreement with experimental results, though there are some small systematic errors.[16,20] It should be noted that hydrogenated Si(100) surface prepared by fluoride etching has significant atomic-scale surface roughness and faceting, resulting in a wide range of surface hydride modes.[21,22] Here we only use the monohydride-terminated Si(100)-(2×1) surface, which has been performed in previous studies of ALD growth mechanism.[23] The Si(100)-(2×1) surfaces with H- and OH-terminated are shown in Figure 1a,b to represent Si−H* and Si−OH* surfaces, respectively.

All the calculations presented in this work have been carried out using the Gaussian 03 suite of electronic structure programs.[24] Electronic structure calculations, transition state investigations, and vibrational frequency predictions have been performed using the B3LYP hybrid density functional, which corresponds to Becke's three-parameter exchange functional (B3) along with the Lee−Yang−Parr gradient-corrected correlation functional (LYP). The B3LYP functional has been used extensively in the past few years to calculate binding and activation energies of organic reactions on semiconductor surfaces using the cluster approximation.[25−27] The performance of this functional in predicting the reaction barriers and energies has been assessed against large thermochemistry and thermochemical kinetics experimental databases. These benchmarks indicate that B3LYP reproduces pretty well reaction enthalpies and atomization energies.[28,29] Gaussian is computationally very efficient employing all electron basis sets so that a 6-31G(d) basis set is employed for all atoms.[29,30] Other basis sets are also used to optimize the transition state in reaction (R1) to estimate the influence of basis sets on the reaction energies given here. The clusters are fully relaxed without any geometrical constraints, which could lead to unphysical structural relaxation.[16,23] Frequency calculations are performed after geometry optimizations to check whether a minimum or a first-order saddle point is reached. All energies reported here include zero-point energy corrections.

3. Results and Discussion

The geometry of $Mg(Cp)_2$ with eclipsed Cp rings is optimized in our work because it has been reported that this structure prevails in the gas phase.[31] The optimized structure of $Mg(Cp)_2$ is shown in Figure 1c. The Mg−Cp distance and Cp−Mg−Cp angle are 2.006 Å and 179.5°, respectively, which is in excellent agreement with the values for gas-phase $Mg(Cp)_2$ (2.008 Å and 180°). These parameters are also consistent with the theoretical results calculated by Rayon and others.[32,33] Moreover, the obtained Mg−C and C−C bond distances (2.363 and 1.423 Å) are also in good agreement with the experimental data for gas-phase $Mg(Cp)_2$ (2.339 and 1.423 Å).

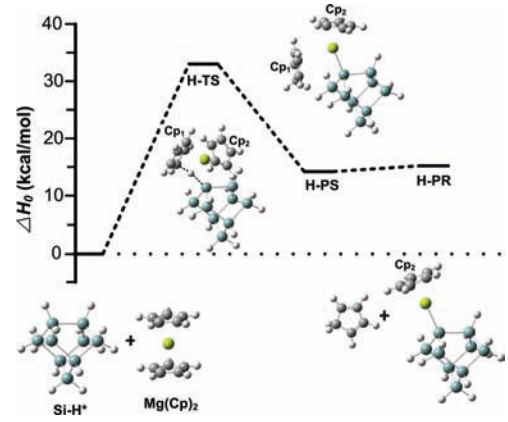

Figure 2. Potential energy surface and optimized geometries for the reaction between gaseous $Mg(Cp)_2$ and the Si−H* surface. Density functional calculations done at the B3LYP/6-31G(d) level of theory.

TABLE 1: Representative Bond Lengths for the Structures of H-TS, H-PS, and H-DS and Reaction Energies at 0 K (ΔH_0) for $Mg(Cp)_2$ + Si−H*[a]

	Mg−Cp_1	Mg−Cp_2	C−H	Mg−Si	Si−H	ΔH_0
H-TS	2.50	2.04	1.48	2.87	1.82	32.7
H-PS	3.63	2.02	1.10	2.57	3.38	14.3
H-PR		1.97		2.55		15.3

[a] All bond lengths are shown in Å, while energies are shown in kcal/mol.

A. Reaction Path for the Adsorption of $Mg(Cp)_2$ on H−Si (100)-(2×1). In this reaction, one of the Cp rings in $Mg(Cp)_2$ abstracts a surface H atom from the surface Si−H* group via the exchange reaction, resulting in the elimination of HCp from the surface, forming the final product state. The potential energy surface (PES) and optimized geometries of the activated complexes of the reaction between $Mg(Cp)_2$ and Si−H* surface species are shown in Figure 2. Representative bond lengths and the corresponding reaction energies (kcal/mol) at 0 K are listed in Table 1. As can be seen, the reaction proceeds without the formation of an initial chemisorbed state. A high activation barrier is needed for the HCp formation. The energy of the transition state (H-TS) relative to the reactants is calculated to be 32.7 kcal/mol. It is found that $Mg(Cp)_2$ has been distorted from its linear equilibrium geometry to a bent geometry upon complexation with Si−H* surface, with a Cp_1−Mg−Cp_2 angle of 150.6°. The Mg−Cp_1 and Si−H bond distances increase from 2.01 and 1.23 Å in the reactants to 2.50 and 1.87 Å in the H-TS, respectively, consisting with the ultimate scission of these bonds. The bond distance between Mg and Si atoms is 2.87 Å, suggesting that the bond is a dative bond. The formation of the physisorbed HCp state (H-PS) is 14.3 kcal/mol endothermic relative to the reactants. The Cp_1−Mg−Cp_2 angle is further

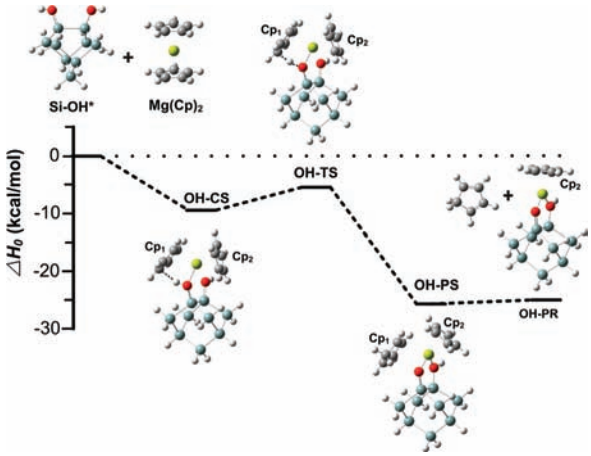

Figure 3. Potential energy surface and optimized geometries for the reaction between $Mg(Cp)_2$ and Si−OH* surface. Density functional calculations done at the B3LYP/6-31G(d) level of theory.

TABLE 2: Representative Bond Lengths for the Structures of OH-CS, OH-TS, OH-PS, and OH-PR and Reaction Energies at 0 K (ΔH_0) for $Mg(Cp)_2$ + Si−OH*[a]

	Mg−Cp_1	Mg−Cp_2	C−H	Mg−O	O−H	ΔH_0
OH-CS	2.55	2.05	1.94	2.06	1.01	–9.0
OH-TS	2.53	2.02	1.40	1.98	1.26	–5.9
OH-PS	3.33	2.01	1.10	1.93	2.60	–26.9
OH-PR		2.01		1.90		–25.1

[a] All bond lengths are shown in Å, while energies are shown in kcal/mol.

decreased to be 122.0° and the Mg−Cp_1 distance is elongated to 3.63 Å in the H-PS. It should be noted that the Cp_1 position of H-PS would not be possible on the extended surface. The energy value for the desorption of the HCp from the surface is only 1.0 kcal/mol, suggesting that it is easy to purge the byproduct out of the reactor. It is not necessary to use a long purge time or oxidant exposure time in the actual ALD process. It means that if the reactants are not thermally accommodated, residual energy can be available to help drive the reaction, effectively increasing the rate of reaction. The Cp_2−Mg−O angle and Mg−O bond length go from 134° and 2.57 Å in the H-PS to 180° and 2.55 Å in the product (H-PR), respectively, indicating complete bond formation. From the PES of the reaction, it is concluded that the adsorption of $Mg(Cp)_2$ on Si−H* surface is neither kinetically nor thermodynamically favorable.

The activation energy for H-TS that separates the reactants from the product is also calculated with 6-311+G(d,p) and LANL2DZ basis sets. The activation energies relative to the reactants are 33.3 and 32.2 kcal/mol, respectively, in good agreement with the value obtained by using the 6-31G(d) basis set. As a result, it is suitable to perform our computations through the combination of the B3LYP functional with 6-31G(d).

B. Reaction Path for the Adsorption of $Mg(Cp)_2$ on OH−Si (100)-(2×1). The PES and optimized geometries of the intermediates for the reaction between $Mg(Cp)_2$ and the Si−OH* surface are shown in Figure 3. As before, Table 2 summarizes the representative bond lengths and the corresponding reaction energies along the reaction pathway. In this case, $Mg(Cp)_2$ first chemisorbs at the Si−OH* site through forming a stable chemical adsorption state (OH−CS). Chemical adsorption complex formation is energetically favorable, with a calculated binding energy of 9.0 kcal/mol lower than the gas-phase reactants. The geometry of $Mg(Cp)_2$ has been bent with a calculated Cp_1−Mg−Cp_2 angle of 156.4° in OH−CS. A significant increase in the Mg−Cp_1 bond length, from 2.01 Å in $Mg(Cp)_2$ to 2.55 Å in OH−CS, also can be found. For another Cp ring, the Mg−Cp_2 distance increases only slightly to 2.05 Å. The Cp_1 ring of the absorbed $Mg(Cp)_2$ then reacts with the H atom of the Si−OH* surface group through a transition state (OH-TS), which is 3.1 kcal/mol higher in energy than that of OH−CS. The angle of Cp_1−Mg−Cp_2 further decreases to 149.0° along with the increasing of O−H bond distance. The calculated Cp_1−Mg−O angle and Mg−Cp_1 bond length in the OH-TS are similar to those in the OH−CS. Over the reaction OH-TS barrier, it leads to a physisorbed state where MgCp* is bonded to the surface through a Mg−O−Si bridge along with the formation of HCp. Mg−O bond formation is evident, with a calculated Mg−O bond length of 1.93 Å. The formation of the physisorbed HCp is 26.9 kcal/mol exothermic relative to the reactants. Desorption of the byproduct HCp from the surface also requires an additional 1.8 kcal/mol. The Mg−O and Mg−Cp_2 bond distances in the final product (OH-PR) are 1.90 and 2.01 Å, which are 0.08 and 0.01 Å less than corresponding lengths in the OH-TS. The overall reaction is exothermic by 25.1 kcal/mol, indicating that the dissociation pathway involving elimination of the Cp group in $Mg(Cp)_2$ through hydrogen loss of the Si−OH* surface is kinetically and dynamically favorable.

A comparison of both pathways suggests that the kinetic barrier required for the breaking of the Mg−Cp bond is much higher for reaction (R1) to occur efficiently. The lack of a chemisorbed state indicates that $Mg(Cp)_2$ has a low reactive sticking coefficient on H-terminated silicon. In contrast, formation of the structure OH-PS has a small kinetic barrier, which suggests that dissociation can take place readily. Moreover, desorption of the HCp from the surface leads to the structure OH-PR that is highly stable in reaction (R2). As a result, the reaction of $Mg(Cp)_2$ with the Si−OH* site will be more prevalent relative to that with Si−H* site. Overall, ALD MgO on H-terminated Si will be slow unless the surface is functionalized with −OH group.

4. Conclusions

In summary, the reaction pathways of $Mg(Cp)_2$ with hydrogenated and hydroxylated Si(100) surfaces have been investigated by density functional theory. For the reaction between $Mg(Cp)_2$ and Si−H* surface, the transition state energy was determined to be 32.7 kcal/mol. The overall reaction is 15.3 kcal/mol endothermic relative to the reactants. The reaction barrier to ligand exchange for $Mg(Cp)_2$ with the Si−OH* group is only 3.1 kcal/mol. Furthermore, the reaction is exothermic by 25.1 kcal/mol relative to the reactants, indicating that the dissociation pathway involving elimination of the Cp ring in $Mg(Cp)_2$ through hydrogen loss of the OH* group on Si surface is kinetically and dynamically favorable. Consequently, it is expected that most initial MgO ALD reactions will proceed through hydrogen transfer from Si−OH*.

Acknowledgment. The work was supported by NSFC (60776017), the Science and Technology Committee of Shanghai under Grant No. 071111007, and the specialized Research Fund for the Doctoral Program of Higher Education (20060246032). The authors would also like to acknowledge the National High Performance Computing Center at Fudan University for computation time.

References and Notes

(1) Burton, B. B.; Goldstein, D. N.; George, S. M. *J. Phys. Chem. C* **2009**, *113*, 1939.

(2) Craft, H. S.; Collazo, R.; Losego, M. D.; Mita, S.; Sitar, Z.; Maria, J.-P. *Appl. Phys. Lett.* **2007**, *102*, 074104.
(3) Miao, G. X.; Chang, J. Y.; van Veenhuizen, M. J.; Thiel, K.; Seibt, M.; Eilers, G.; Munzenberg, M.; Moodera, S. *Appl. Phys. Lett.* **2008**, *93*, 142511.
(4) Kawakami, A.; Uzawa, Y.; Wang, Z. *Appl. Phys. Lett.* **2003**, *83*, 3954.
(5) Arendt, P. N.; Foltyn, S. R. *MRS Bull.* **2004**, *29*, 543.
(6) Jung, H. S.; Lee, J.-K.; Hong, K. S.; Youn, H.-J. *J. Appl. Phys.* **2002**, *92*, 2855.
(7) Yan, L.; Lopez, C. M.; Shrestha, R. P.; Irene, E. A.; Suvorava, A. A.; Saunders, M. *Appl. Phys. Lett.* **2006**, *88*, 142901.
(8) Casey, P.; Hughes, G.; O'Connor, E.; Long, R. D.; Hurley, P. K. *J. Phys.: Conf. Ser.* **2008**, *100*, 042046.
(9) Carta, G.; Habra, N. E.; Crociani, L.; Rossetto, G.; Zanella, P.; Zanella, A.; Paolucci, G.; Barreca, D.; Tondello, E. *Chem. Vap. Deposition* **2007**, *13*, 185.
(10) Cheng, Y. H.; Hupfer, H.; Richter, F.; Paraian, A. M. *Appl. Surf. Sci.* **2002**, *200*, 117.
(11) Yoon, J. G.; Kim, K. *Appl. Phys. Lett.* **1995**, *66*, 2661.
(12) Huang, R.; Kitai, A. H. *Appl. Phys. Lett.* **1992**, *61*, 1450.
(13) Putkonen, M.; Johansson, L. S.; Rauhala, E.; Niinisto, L. *J. Mater. Chem.* **1999**, *9*, 2449.
(14) Putkonen, M.; Sajavaara, T.; Niinisto, L. *J. Mater. Chem.* **2000**, *10*, 1857.
(15) Rodriguez-Reyes, J. C. F.; Teplyakov, A. V. *Chem.—Eur. J.* **2007**, *13*, 9164.
(16) Halls, M. D.; Raghavachari, K. *J. Phys. Chem. B* **2004**, *108*, 4058.
(17) Jeloaica, L.; Esteve, A.; Rouhani, M. D.; Esteve, D. *Appl. Phys. Lett.* **2003**, *83*, 542.
(18) Willis, B. G.; Mathew, A.; Wielunski, L. S.; Opila, R. L. *J. Phys. Chem. C* **2008**, *112*, 1994.
(19) Widjaja, Y.; Han, J. H.; Musgrave, C. B. *J. Phys. Chem. B* **2003**, *107*, 9319.
(20) Fattal, E.; Radeke, M. R.; Reynolds, G.; Carter, E. A. *J. Phys. Chem. B* **1997**, *101*, 8658.
(21) Frank, M. M.; Chabal, Y. J.; Wilk, G. D. *Appl. Phys. Lett.* **2003**, *82*, 4758.
(22) Leftwich, T. R.; Madachik, M. R.; Teplyakov, A. V. *J. Am. Chem. Soc.* **2008**, *130*, 16216.
(23) Halls, M. D.; Raghavachari, K.; Frank, M. M.; Chabal, Y. J. *Phys. Rev. B* **2003**, *68*, 161302.
(24) Frisch, M. J.; Trucks, G. W.; Schlegel, H. B.; Scuseria, G. E.; Robb, M. A.; Cheeseman, J. R.; Montgomery, J. A.; Vreven, T., Jr.; Kudin, K. N.; Burant, J. C.; Millam, J. M.; Iyengar, S. S.; Tomasi, J.; Barone, V.; Mennucci, B.; Cossi, M.; Scalmani, G.; Rega, N.; Peterson, G. A.; Nakatsuji, H.; Hada, M.; Ehara, M.; Toyota, K.; Fukuda, R.; Hasegawa, J.; Ishida, M.; Nakajima, T.; Honda, Y.; Kitao, O.; Nakai, H.; Klene, M.; Li, X.; Knox, J. E.; Hratchian, H. P.; Cross, J. B.; Bakken, V.; Amado, C.; Jaramillo, J.; Gomperts, R.; Stratmann, R. E.; Yazyev, O.; Austin, A. J.; Cammi, R.; Pomelli, C.; Ochterski, J. W.; Ayala, P. Y.; Morokuma, K.; Voth, G. A.; Salvador, P.; Dannenberg, J. J.; Zakrzewski, V. G.; Dapprich, S.; Daniels, A. D.; Strain, M. C.; Farkas, O.; Malick, D. K.; Rabuck, A. D.; Raghavachari, K.; Foresman, J. B.; Ortiz, J. V.; Cui, Q.; Baboul, A. G.; Clifford, S.; Cioslowski, J.; Stefanov, B. B.; Liu, G.; Liashenko, A.; Piskorz, P.; Komaromi, I.; Martin, R. L.; Fox, D. J.; Keith, T.; Al-Laham, M. A.; Peng, C. Y.; Nanayakkara, A.; Challacombe, M.; Gill, P. M. W.; Johnson, B.; Chen, W.; Wong, M. W.; Gonzalez, C.; Pople, J. A. *Gaussian 03*, revision D.02; Gaussian, Inc.: Wallingford, CT, 2004.
(25) Kelly, M. J.; Han, J. H.; Musgrave, C. B.; Parsons, G. N. *Chem. Mater.* **2005**, *17*, 5305.
(26) Lu, H. L.; Chen, W.; Ding, S. J.; Zhang, D. W.; Wang, L. K. *J. Phys. Chem. B* **2006**, *110*, 9529.
(27) Lu, H. L.; Xu, M.; Ding, S. J.; Chen, W.; Zhang, D. W.; Wang, L. K. *Appl. Phys. Lett.* **2006**, *89*, 162905.
(28) Guner, V.; Khuong, K. S.; Leach, A. G.; Lee, P. S.; Bartberger, M. D.; Houk, K. N. *J. Phys. Chem. A* **2003**, *107*, 11445.
(29) Hall, M. A.; Mui, C.; Musgrave, C. B. *J. Phys. Chem. B* **2001**, *105*, 12068.
(30) Lu, H. L.; Chen, W.; Ding, S. J.; Xu, M.; Zhang, D. W.; Wang, L. K. *J. Phys.: Condens. Matter* **2005**, *17*, 7517.
(31) Haaland, A.; Lusztyk, J.; Brunvoll, J.; Starowieyski, K. B. *J. Organomet. Chem.* **1975**, *85*, 279.
(32) Rayon, V. M.; Frenking, G. *Chem.—Eur. J.* **2002**, *8*, 4693.
(33) Wang, G. T.; Creighton, J. R. *J. Phys. Chem. A* **2004**, *108*, 4873.

JP904048D